Indian J. Phys. 77A (5), 425–431 (2003)

AN INTERNATIONAL JOURNAL
IJPA

Dielectric and impedance spectroscopic studies on nanophase silver orthophosphate

Marykutty Thomas[1], S K Ghosh[2] and K C George*
Department of Physics, SB College, Changanacherry-686 101, Kerala, India
[1]Department of Physics, BCM College, Kottayam-686 001, Kerala, India
[2]Ceramics Division, RRL, Trivandrum-695 019, Kerala, India
E-mail : ktm_kcgeorge@sancharnet.in

Received 11 March 2003, Accepted 12 June 2003

Abstract : Nanophase Ag_3PO_4 was prepared by chemical precipitation for three reactant concentrations (0.015 mol.L^{-1}, 0.01 mol.L^{-1}, 0.005 mol.L^{-1}) Room temperature impedance spectroscopic analysis of the samples was carried out using the 'sand witch' geometry. The experimental data for the samples represented by the complex plane diagrams showed three semicircular arcs similar to that of polycrystalline, ionic conductors Dielectric constant (ε) and loss tangent (tan δ) were measured as a function of temperature (300 K–500 K) at different frequencies (100 KHz–10 MHz) Space charge polarization effects are found to be prominent at low frequencies and at high temperatures, characteristic of nanophase materials. Reactant concentration plays a role in determining the electrical properties of nanophase Ag_3PO_4

Keywords : Silver orthophosphate, nanophase materials, impedance spectroscopy, dielectric behaviour, SEM image.

PACS Nos : 61.46.tw, 77.22.Gm, 68.37.Hk

1. Introduction

Nanophase and nanostructured materials, a new branch of material research, are attracting a great deal of attention because of their potential applications in areas such as electronics, optics, catalysis, ceramics, magnetic data storage and nanocomposites [1,2]. The unique properties and the improved performances of nanomaterials are determined by their sizes, surface structures and interparticle interaction [1].

Today different metal phosphates, especially transition metal phosphates are used in many applications such as pigments, catalysts, adsorbents and bioceramic materials [3]. Since characterisation and frequency dependant dielectric behaviour of nanophase Ag_3PO_4 is reported by us [4], we have carried out impedance spectroscopic analysis and temperature dependant dielectric behaviour to know more about the physical property of this material. In nanophase materials, the majority of atoms, molecules or ions reside in the grain boundaries or within one or two layers from the boundary. These grain boundaries having high density of defects like vacancies, dangling bonds, micropores *etc.* can control the transport properties of the materials in a decisive manner [5]. The variation of dielectric constant with temperature can give information about the ferroelectric/diffused phase or any other transition of the material and on the behavior of localized electric charge carriers leading to greater understanding of the mechanism of dielectric polarization. From room temperature dielectric measurements, it is found that nanophase Ag_3PO_4 is a dielectric relaxor material having high value of dielectric constant [4].

Depending upon the concentration of the reacting components, duration and temperature, the precipitated particles may vary in size, shape and uniformity [3,6] and hence the physical properties. Enhanced electrical properties of nanophase materials compared to their bulk counterparts

*Corresponding Author

have been reported in the literature [7,8]. For example, nanophase AgI has been found to have high ionic conductivity compared to its bulk counterpart due to the defect structure of nanoparticles [9]. It is reported that nanoparticle CaF_2 possess an increase in conductivity compared to single crystalline CaF_2 by more than four orders of magnitude [10]. In nanostructured yttria stabilized zirconia, increased ionic conductivity was observed [11]. In the case of nanophase Ag_2HgI_4, increase in ε, tan δ and σ_{ac} was reported compared to polycrystalline pellets of Ag_2HgI_4 [7]. Hence, the study of the effect of reactant concentration on the electrical behaviour of nanoparticle aggregates is relevant. The morphology and the random network connection of nanoparticle aggregates have a considerable role in the transport properties and mechanical restoring force [12]. The morphology can be studied using SEM imaging.

Impedance spectroscopy (IS) is an appropriate experimental technique to obtain information about the electrical characteristics of polycrystalline materials and nanomaterials [5,13]. The techniques probe the electrical response as a function of frequency, of components, the grains and grain boundaries [13]. This method can advantageously be used to study the electrical properties of grain boundaries of nanomaterials. This technique is capable of revealing the structural uniformity, variation in electrical conduction paths, stability *etc.*[5]. IS can be effectively used to study the inter granular electrical barriers, origin of resistance or capacitance and their dispersion with small signal frequencies and the role of defects within the regime of the electric field [14]. The analysis of this response can be used to determine the frequency dependence of the electrical parameters and relate them with the microstructure of polycrystalline material. For that it is necessary to find the equivalent electrical circuit which best fit the electrical response. To find the equivalent circuit, we can look upon Maxwell-Wagner two-layer equivalent circuit model [14]. The overall dielectric properties arise due to intragrain, intergrain and electrode processes in the nanophase materials. The motion of charges could take place in any fashion, *viz* charge displacements, dipole re-orientation, space charge formation *etc.* [14,15]. In order to achieve reproducibility and to have a control over the properties, these so called grain, grain boundary and electrode contribution must be separated out.

The magnitude and temperature variation of *a.c.* conductivity in ionic crystals and glasses is still of great interest [16]. When we consider the dielectric behaviour of a ceramic material, the two factors that are of practical interest are frequency range and the range of environmental conditions, particularly temperature. The temperature dependence of a.c. conductivity points to the existence of various relaxational contributions characterised by different activation energy [16]. Since the frequency dependent dielectric behaviour of nanophase Ag_3PO_4 is already reported [4], we have tried to carry out the temperature dependent dielectric behaviour and room temperature IS studies to understand the basic electrical nature of this material which are hitherto not reported.

2. Experimental

Synthesis and characterisation part of nanophase Ag_3PO_4 is reported by us [4]. SEM image of 0.01 mol.L^{-1} reactant concentration sample was taken using Philips Electron Scanning Electron Microscope XL 30. For IS and dielectric measurements, powder samples were made into pellets of diameter 12 mm and 1–2 mm thickness by applying pressure ~0.5 GPa and the density of the samples was found to be ~72% of theoretical value. The IS and dielectric measurements were carried out using 4192 A LF impedance analyser.

3. Results and discussion

The morphological features of nanophase Ag_3PO_4 of 0.01 mol.L^{-1} concentration can be studied from the SEM image (Figure 1). The figure shows that the clusters are in the form of fractal aggregates [4] and each particle is oval shaped and the aggregate as a whole have a fluffy nature with considerable porosity. Since the material is porous, having large volume of interface, the dielectric behaviour of nanophase Ag_3PO_4 may be different in some respects from conventional materials. The low density of the samples (72%) may also affect the dielectric properties and some changes from conventional materials can be expected.

Figure 1. SEM image of 0.01mol.L^{-1} Ag_3PO_4.

The method of Complex Impedance Analysis (CIA) can be used as a powerful tool for separating out grain, grain boundary and electrode contribution in the case of nanophase materials [5]. In this method, the imaginary part Z'' of the total complex impedance $Z = Z' - jZ''$ of the sample is plotted as a function of the corresponding real part Z' at different frequencies. This plot shows different features depending upon various relative contributions from grain, grain boundary and sample-electrode interface [14].

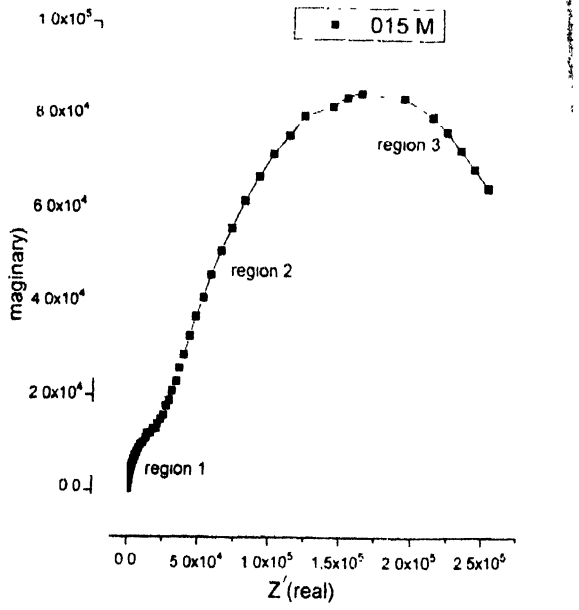

Figure 2a. Impedance spectrum of 0.015mol.L^{-1} Ag_3PO_4.

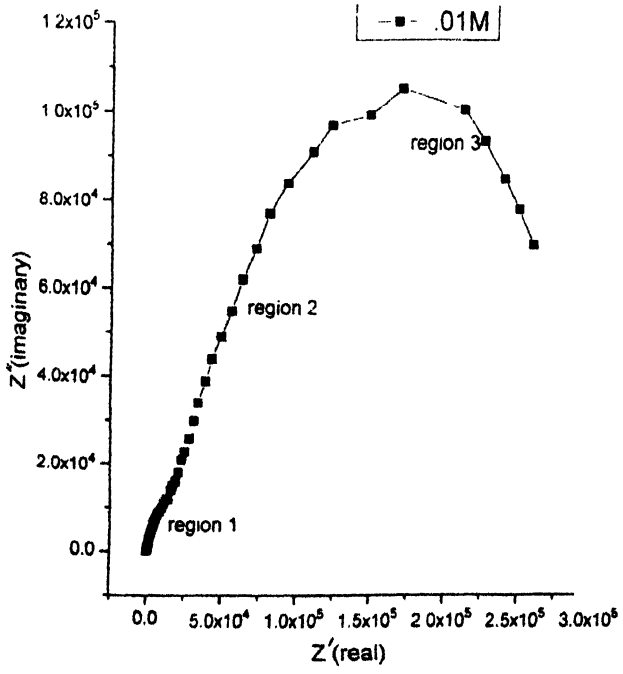

gure 2b. Impedance spectrum of 0.01mol.L^{-1} Ag_3PO_4.

Figures 2a, 2b, and 2c give the impedance spectra obtained at room temperature for nanophase Ag_3PO_4 having reactant concentrations 0.015 mol.L^{-1}, 0.01 mol.L^{-1} and 0.005 mol.L^{-1} respectively. We can observe three

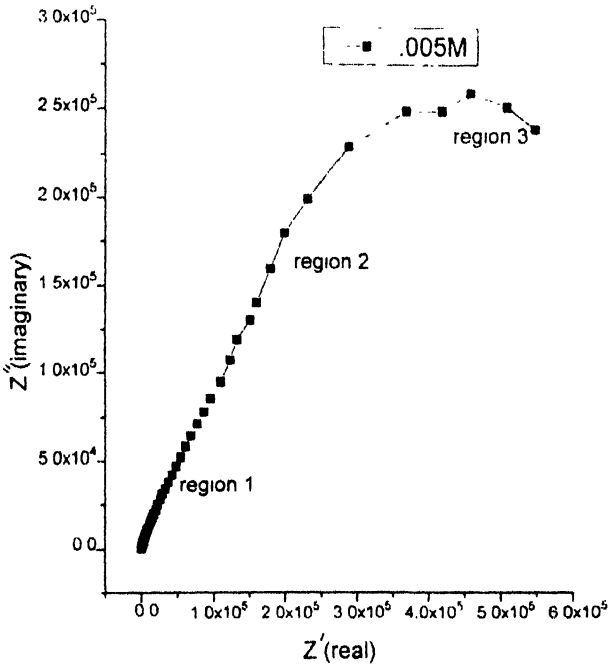

Figure 2c. Impedance spectrum of 0.005mol.L^{-1} Ag_3PO_4.

semi-circular arcs (regions 1, 2 and 3) corresponding to three different relaxation processes in the grains, grain boundaries and sample-electrode interfaces. The contribution of each of these components can be represented by a suitable combination of resistance and capacitance in parallel. The sample can thus be represented by an equivalent circuit (Figure 3) containing three, parallel

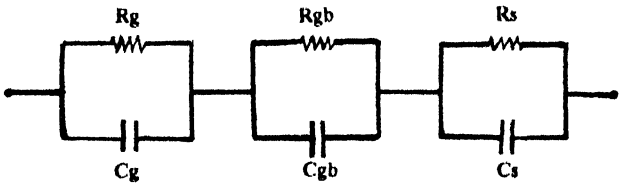

Figure 3. Equivalent electrical circuit model for the impedance spectrum of Ag_3PO_4 corresponding to grain (*Rg, Cg*), grain boundary (*Rgb, Cgb*) and sample-electrode interface (*Rs, Cs*).

R-C element connected in series. The appearance of three overlapping semi-circular arcs in this plot indicates the presence of three polarization processes in the system with different response times, the grain response being at the high frequency side and electrode response at low frequency side. One parallel *R-C* circuit has one time constant and hence can be conveniently used a model to represent one polarization process. The Z' *vs* Z'' plot for

such a *R-C* model containing semi-circular arcs with its intercept on the Z' axis gives resistance value R for each element. Capacitance values can be calculated by using the relation $\omega RC = 1$, where $\omega = 2\pi f$, f being the frequency corresponding to the maximum of each circular arc. A depressed circular arc in the impedance plot with its center of curvature below the Z' axis shows a distribution of relaxation times for the above-mentioned process [5]. Thus, *Rg*, *Rgb* and *Rs* represent grain resistance, grain boundary resistance and sample electrode resistance respectively. Then, the capacitance *Cg*, *Cgb* and *Cs* can be calculated. The contribution to the conductivity due to grain (σ_g) was calculated by measuring the dimensions of the pellets. The mean relaxation time for the grain and the grain boundary processes $\tau g = RgCg$ and $\tau gb = RgbCgb$ are the inverse of the peak frequencies ωg and ωgb.

The overall impedance behaviour of the three samples is mainly constituted of the contributions from the grain boundaries and the impurity phases may be present at the grain boundaries. The intergranular porosity largely alters the diameter of the grain boundary arc (*Rgb*) in the impedance spectrum as shown in Figure 2 (region 2). The diameter of the semi circle (region 1), a measure of the grain contribution to the total resistivity (*Rg*) is comparatively small in all the three samples. The grain contribution to the impedance spectrum by three-molarity samples is given in Table 1. Since the grain boundary

Table 1. Variations of grain resistance, grain capacitance and grain conductivity with reactant concentration

mol.L^{-1}	*Rg* (Kilo ohm)	*Cg* (pF)	σg (ohm^{-1} m^{-1})
0.015	36.5	77.6	2.550E-4
0.01	112	42.4	0.935E-4
0 005	250	22.5	0.404E-4

resistance *Rgb* (intercept of region 2) is very large compared with grain resistance, conductivity is mainly through grains, which is characteristic of ionic conductors [17]. Grain conductivity decreases with decreasing reactant concentration, which may be due to decrease in particle size. Since in the nanoparticles, the surface atoms will have higher diffusion coefficient than that of the bulk, we normally expect higher conductivity and lower activation energy. But in the present study, the lesser conductivity in the grain boundaries may be due to the impurity phases, porosity and large area of grain boundary region [17]. The low value of conductivity in 0.005 mol.L^{-1} sample compared to other two samples may be due to the confined passage of the Ag^+ ions within the small grains. The ionic conductivity is directly proportional to the jump attempt frequency and the square of the jump distance. The jump attempt frequency may be smaller in lower concentrated samples resulting in lower conductivity [17].

Figure 4 shows the variation of dielectric constant with temperature for 0.01 mol.L^{-1} sample at different frequencies.

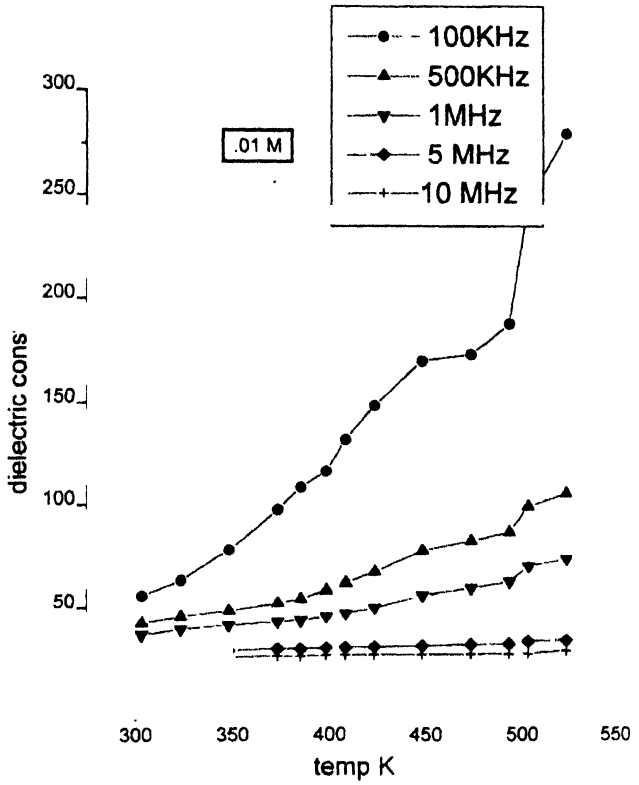

Figure 4. Variation of dielectric constant ε with temperature for 0.01mol.L^{-1} Ag_3PO_4.

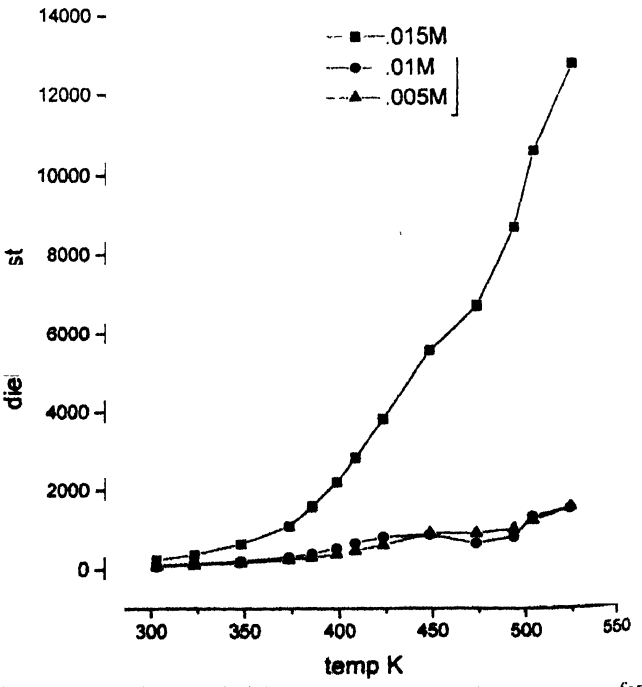

Figure 4a. Variation of dielectric constant ε with temperature for 0.015mol.L^{-1}, 0.01mol.L^{-1}, 0.005mol.L^{-1} samples at 10 KHz.

The same pattern is obtained for other two concentrations of the sample, with the value of the dielectric constant minimum for 0.005 mol.L^{-1} which is having lowest particle size [4]. At higher temperatures, there is an increasing contribution resulting from ion mobility and crystal imperfection mobility. Also at higher temperatures, *d.c.* conductivity effects, which increase exponentially with temperature, become important. The combined effect is to give a sharp rise in the apparent dielectric constant at low frequencies with temperature, corresponding to both ion jump orientation effects and space charge effects resulting from the increased concentration of charge carriers [18]. The defect concentration increases with temperature and at a particular high temperature, the charges get depleted resulting in a peak [19]. This may be due to the fact that the charges can get over the potential barrier set up by the regions of charge accumulation. There is a shift in the peak positions with higher frequencies with increasing temperature for all the samples, which are characteristic of ionic conductors [19]. A high value of dielectric constant ε of nanophase materials is closely related to space charge polarisation and rotation direction polarisation [20]. The characteristic of space charge polarisation and rotation direction polarisation is the appearance of peak in the spectrum of ε *vs* T (temperature). In our case, this effect is stronger at low frequencies. Figure 4a shows ε *vs* T at 10 KHz for different concentration samples indicating low value for 0.005 mol.L^{-1}.

Figure 5 shows the variation of loss tangent (tan δ) with temperature for different frequencies for 0.01 mol.L^{-1} sample in which a pattern similar to ε *vs* T is obtained. In nanophase materials, inhomogeneties like defects, space charge formation *etc.* in the interphase layers together produce an absorption current resulting in a dielectric loss. Also enhancement in *d.c.* conductivity will give rise to currents which in an *a.c.* field are in phase with applied voltage and hence cause dielectric loss [21]. The variation of loss tangent with temperature (Figure 5) shows a smooth increasing trend at high frequencies whereas at low frequencies, there is a peak around 172°C and this peak shifts towards higher temperature as frequency increases. Figure 5a shows tan δ *vs* T for three molarity samples indicating tan δ minimum for 0.005 mol.L^{-1} sample and there is a cross over at 172°C for 0.01 mol.L^{-1} and 0.005 mol.L^{-1}, which may be due to the structure of nanophase materials.

Figure 6 shows the Arrhenius plot for the a.c. conductivity of the samples at frequencies 10 KHz (low frequency) and 1 MHz (high frequency). The temperature variation of a.c. conductivity σ can be written as $\sigma T = \sigma 0 \exp(-Ea/K_bT)$, where Ea = a.c. activation energy, K_b=

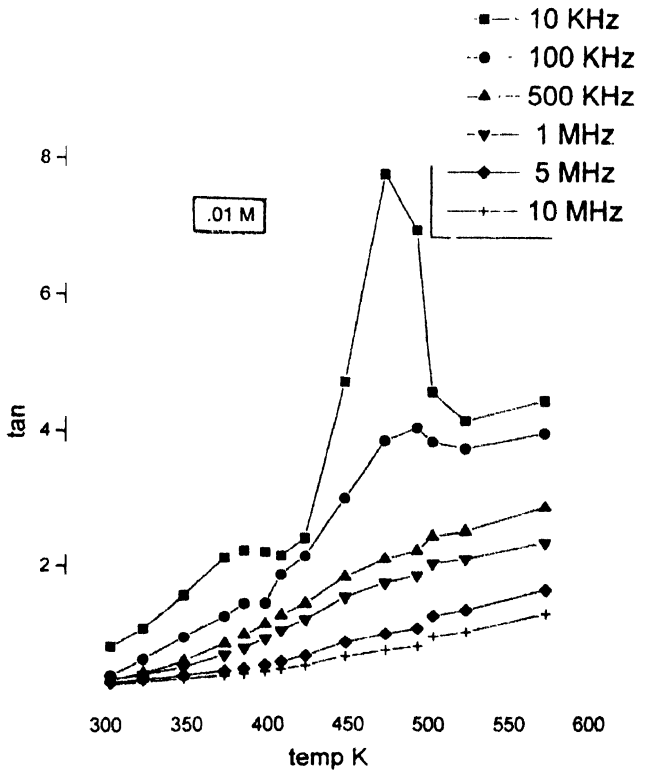

Figure 5. Variation of loss tangent tan δ with temperature at different frequencies for 0.01mol.L^{-1} Ag_3PO_4.

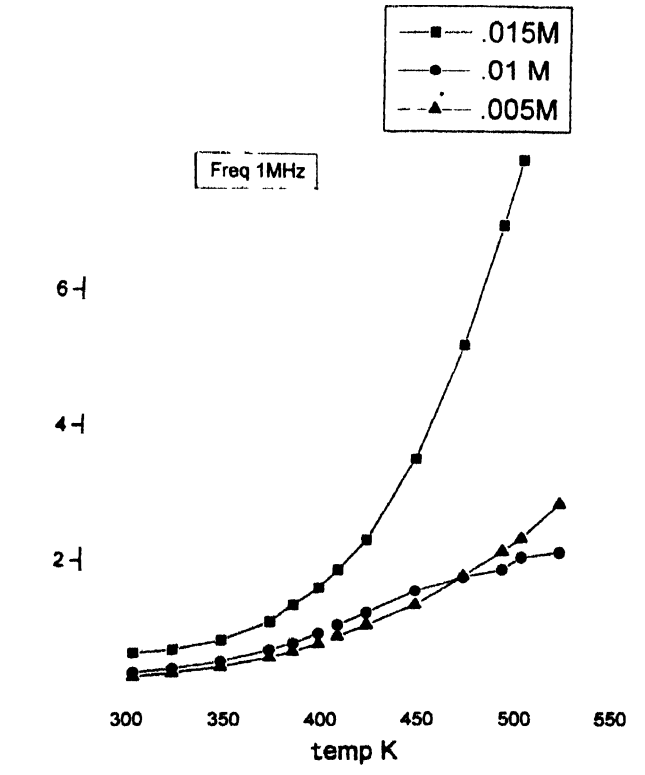

Figure 5a. Variation of loss tangent with temperature for 0.015mol.L^{-1}, 0.01mol.L^{-1}, 0.005mol.L^{-1} samples.

Boltzmann constant, $\sigma 0$ = the pre-exponential factor. Experimental data was compared with straight line fit and the values of pre-exponential factor σo and activation energy *Ea* calculated from the slope of the straight line are given in Table 2. The molecular environments in which the

Table 2. Variation of activation energy and pre-exponential factor with reactant concentration

	Frequency 1 MHz		Frequency 10 KHz	
mol.L^{-1}	Activation energy (eV)	Pre-exponential factor (ohm^{-1}m^{-1}K)	Activation energy (eV)	Pre-exponential factor (ohm^{-1}m^{-1}K)
0.015	0.0842	2.568	0.1128	3.1025
0.01	0.0886	2.587	0.1419	3.542
0.005	0.0992	2.783	0.1529	3.763

molecular motion takes place, cause the pre-exponential factor. This factor is important in nanoparticles which is a defect structure, and the conductivity depends on this factor too. Space charge effects play an important role in controlling the electrical properties of very small crystals since the grain boundaries contain a large number of defects compared to its bulk materials. From Figure 6, we can observe that a.c. conductivity is frequency dependant as well as temperature dependant. Also for a given frequency, conductivity is found to be minimum for low molarity sample (0.005 mol.L^{-1}). The conductivity minimum for lower concentration sample may be due to smaller size of the grains compared to other two samples. It is reported that conductivity is minimum in smaller grains due to the confined passage of the conducting species with in the grains due to its smallness [17]. Arrhenius plot shows that the slope change observed at higher temperature (172°C) may be attributed to the sudden release of space charges, which get accumulated at the grain boundaries [19,22]. In this region, there is a decrease in activation energy where space charge polarisation effect is dominant and d.c. conductivity effect starts [22]. There are different reports attributing different causes to the change of activation energy, such as trapping of oxygen vacancies, defect interactions, formation of vacancy clusters, space charge layers *etc.* at lower temperatures [17]. In our case, for 0.015 mol.L^{-1} sample having large particle size, there is no decrease in activation energy at higher temperature. But in the case of 0.01 mol.L^{-1}and 0.005 mol.L^{-1} sample, there is slight decrease in activation energy at higher temperature. This may be due to the dissociation of the vacancy clusters and defects (space charge polarisation) and this polarisation effect is found to be small in larger particles (0.015 mol.L^{-1}). From Table 2, we can observe that *Ea* and $\sigma 0$ change with frequency and is slightly lower in high frequency samples compared with low frequency. Since nanophase Ag_3PO_4 is a frequency dependent dielectric material [4], activation energy and pre-exponential

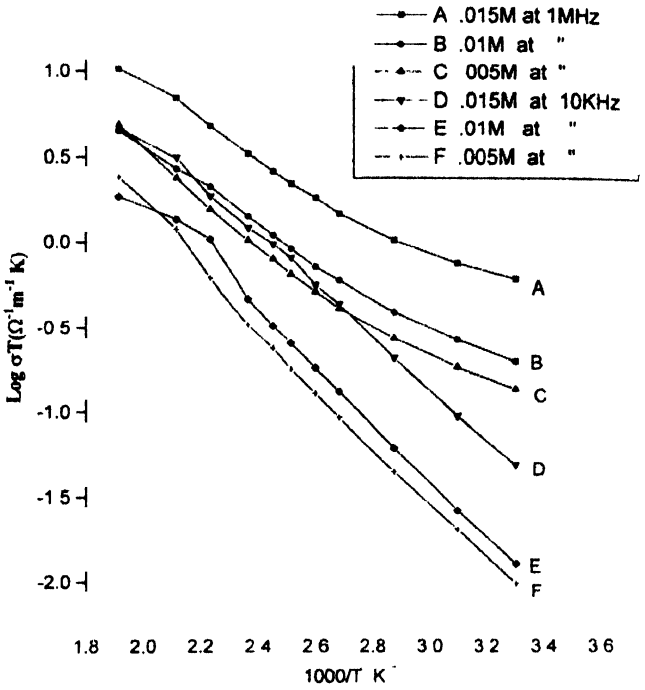

Figure 6. Arrhenius plot for the a c conductivity at 10 KHz and 1 MHz

factor may slightly vary with frequency. Reactant concentration also affects the value of *Ea* and $\sigma 0$ which may depend on the particle size.

4. Conclusion

The SEM image shows that the material is porous, having large volume of interface which makes the dielectric behaviour of nanophase Ag_3PO_4 to differ obviously in some respects, from conventional materials. The dielectric anomaly observed in the case of nanophase Ag_3PO_4 at high temperatures and low frequencies is due to space charge polarisation effects, which are characteristic of nanophase materials. From IS study and dielectric behaviour it is observed that at low frequencies, grain boundary effects are prominent and at high frequencies grain (bulk) conductivity effects (ionic conductivity) are important. The reactant concentration, which plays a role in determining the grain size, has a considerable role in determining the properties of materials.

References

[1] Zhong Lin Wang (ed) *Characterisation of Nanophase Materials* (New York : Wiley-Vch) (2000)

[2] Harisingh Nalwa (ed) *Hand book of Nanostructured Materials and Nano Technology* (New York : Academic) **Vol.1** (2000)

[3] Tatsuo Ishikawa and Egon Matijevic *Colloid Interface Sci.* **123** 122 (1988)

[4] Marykutty Thomas, S K Ghosh and K C George *Mater Lett.* **56** 386 (2002)

[5] Joshy Jose and M Abdul Khadar *Nanostructured Materials* **11** 1091 (1999)

[6] Ruitao Wu, Yu Wei and Yanfeng Zhang *Mater. Res Bull.* **34** 2131 (1999)

[7] S Sankara Narayanan Potty and M Abdul Khadar *Bull Mater Sci.* **23** 361 (2000)

[8] Y M Chiang, E B Lavik and D A Bloom *Nanostructured Materials* **9** 633 (1997)

[9] M Abdul Khadar and Binny Thomas *Bull Mater Sci* **19** 631 (1995)

[10] W Puin and P Heitjans *Nanostructured Materials* **6** 885 (1995)

[11] R Ramamoorthy, R W Viswanath and S Ramasamy *Nanostructured Materials* **6** 337 (1995)

[12] Armin Bunde and Shlomo Havlin (eds) *Fractals and Disordered Systems* (2nd edn. Springer) (1995)

[13] M B Ortuno-Lopez, J J Valenzuela-Jauregui, R Ramirez-Bon, E Prokhorov, J and Gonzalez-Hernandez *Phys. Chem Solids* **63** 665 (2002)

[14] J R Mac Donald (ed) *Impedance Spectroscopy, Emphasizing Solid Materials and Systems* (New York : John Wiley) (1987)

[15] Lakshman Pandey, O M Parkash, Rejesh K Katare and Devendra Kumar *Bull Mater Sci* **18** 563 (1995)

[16] M Cutroni, A Mandanici, A Piccolo, C Fanggao, G A Saunders and P Mustrelli *Solid State Ionics* **90** 167 (1996)

[17] R Ramamoorthy, D Sundararaman and S Ramasamy *Solid State Ionics* **123** 271 (1999)

[18] W D Kingery *Introduction to Ceramics* (New York John Wiley) (1976)

[19] M Mahesh Kumar, A Srinivas and S V Suryanarayana *Phys Stat Sol* (*a*) **165** 317 (1998)

[20] Mo Chi-mei, Zhang Lide and Wang Guozhong *Nanostructured Materials* **6** 823 (1995)

[21] B Tareev *Physics of Dielectric Materials* (Moscow : Mir) (1979)

[22] Tanika Kar, R N P Choudhary, Seema Sharma and K S Singh *Indian J Phys* **73A** 453 (1999)